A Novel Hybrid Car Design using a Wind Energy Capturing Device

Su-Huei Chang
Department of industrial Education
National Taiwan Normal University
Taipei, Taiwan
s07838@gmail.com

Qi-Hong Lim
Mechanical and Manufacturing Engineering
The University of New South Wales
Sydney, Australia
qihong88@gmail.com

Kuo-Hsin Lin
Department of Industrial Technology
Dong Fang Vocational High School
Taipei , Taiwan
lks@tfvs.tp.edu.tw

***Abstract*—Due to the scarcity of fossil fuel in the future and its detrimental effect on the environmental, an alternative energy has to be discovered. Wind power is a clean and sustainable natural resource that has yet to be fully utilised in the automotive industry. The possibility of using a wind turbine on a vehicle was explored. However, the efficiency of a conventional wind turbine is limited. Therefore, a wind turbine system that consists of a diffuser shroud with a curved flange at the exit periphery was developed to overcome these weaknesses. The curve-flanged diffuser shroud has the role of collecting and accelerating the approaching wind, thus improving the efficiency of the wind turbine. In the numerical simulation, it was found that the curve-flanged diffuser shroud could accelerate the approaching wind speed by a factor of 2.1 and augment the power output of a wind turbine by 3 times. However, in the wind tunnel experiment, a velocity enhancement of 1.33 times was achieved and a power output augmentation of 2 times was demonstrated.**

Keywords- Wind Turbine, Alternative Energy, Diffuser Shroud

I. INTRODUCTION

Fossil fuel combustion, particularly as it occurs in motor vehicles, has been identified as the largest contributor to air pollution in the world. The biggest disadvantage of burning fossil fuel is the by-product, carbon dioxide, which leads to a greenhouse effect that harms the planet. According to the United States Environmental Protection Agency (EPA, 2007), a conventional family car emits approximately four tonnes of carbon dioxide per year, while as much as six tonnes of carbon dioxide is emitted by a van or four wheel drive vehicle yearly. However, it took the society years to realise the deterioration of the planet. The excess of greenhouse gases could cause the extinction of animal species, loss of health and global warming, leading to environmental problems. Additionally, the amount of petroleum remaining is depleting rapidly due to its high demand around the world. Some scientists claim that the oil reserve could run out in the next 60 years (EIA, 2011). As a result, people are becoming more aware of the energy related actions and have started looking for an alternative sustainable source.

The use of wind energy started as early as 3000 B.C. through the use of sail boats. The sails captured the wind energy to pull a boat across the water. In the 21st Century, wind turbine vehicles were introduced. A modern example is the Wind-explorer, a lightweight vehicle solely powered by wind generated electricity. In 2011, the Wind-explorer travelled within Australia for more than 5000 km by wind turbine at just eight meters in height and three meters in rotor diameter to charge its battery. However the battery can only be charged when the car is not operating.

Through the example, the idea for the use of a portable wind turbine on a vehicle was obtained. This is because when a car is moving forward, the amount of wind that can be harnessed is unlimited. By installing a wind energy capturing device, wind energy can be obtained regardless during day or night. Moreover, the low maintenance cost after initial procurement coupled with long term and sustainable energy provision leads to the possibility of a wind powered hybrid vehicle.

II. LITERATURE REVIEW

A. Literature Review and Theory

1.Wind Turbine

A wind turbine is a device, which converts wind power into electricity. It is usually connected to network consisting of battery charging circuits, residential scale power systems, and large utility grids. In modern wind turbines, the actual conversion process uses the basic aerodynamic force of lift to produce a net positive torque on a rotating shaft, resulting in the production of mechanical power. It is then transformed into electrical power by a generator. The conventional wind turbines can be classified into two main types: the horizontal axis wind turbines (HAVT) and the vertical axis wind turbines (VAHT). Furthermore, a separate category commonly known as the “ wind energy concentrators” or “shrouded wind turbines” have been investigated and developed to increase the power of wind turbine.

2.Horizontal Axis Wind Turbine (HAWT)

In a HAWT, the shaft is mounted horizontally, parallel to the ground. A yaw-adjustment mechanism is usually applied, as the rotor axis of HAWT needs to be constantly aligned with the wind direction. By controlling the pitch angle of the rotor blades along their longitudinal axis, the desired rotor speed as well as the power output can be adjusted. This pitch control mechanism provides effective protection against over-speed and extreme wind conditions. In addition, the rotor blade shape can be aerodynamically optimised to achieve the highest efficiency in extracting wind power. For HAWT, especially large model, there is a support structure named "tower" that is attached to the foundation buried in the ground to keep the wind turbine aligned with the approaching wind.

3.Vertical Axis Wind Turbine (VAWT)

In a VAWT, the rotor shaft is mounted vertically, perpendicular to the ground. Unlike HAWT, yaw system is not installed in VAWT, as they can receive wind from any direction. However, a VAWT does not start rotating on its own and requires a boost from its electrical system to get started. A typical VAWT uses wire for support instead of the tower, therefore the rotor elevation is lower. Lower elevation means slower wind due to ground interference, so in general VAWTs are less efficient than HAWTs. On the upside, all equipment is at ground level for easy installation and servicing. The general component of a VAWT is shown in Figure 1.

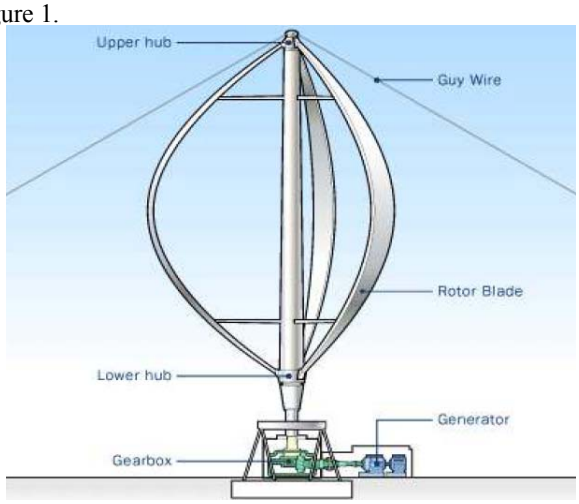

Figure 1. Vertical Axis Wind Turbine (Jha, 2011)

3.Wind Energy Concentrators

The basic concept of wind energy concentrators shown in Figure 2 is to increase the power yield in relation to the rotor swept area. This can be achieved through the use of a static structure named "shroud" which produces acceleration in the flow velocity to the rotor. In some cases, the design of the shroud can even generate concentrating vortices and thus increase the power yield (Hau, 2006).

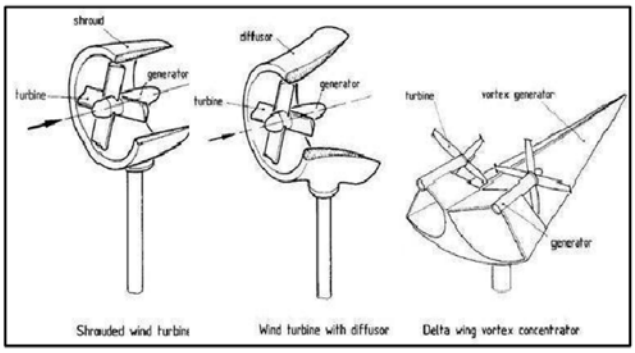

Figure 2. Wind Energy Concentrator Structure (Hau, 2006)

4. Efficiency Improvement of Wind Turbine

Betz figured out that the wind power capture ability of a bare rotor can never exceed 0.59 of the available energy from the wind (Betz, 1966). Many researches have been done to overcome this limitation. In this section, a brief explanation of wind turbine technology will be presented, as well as the feasibility of these technologies on vehicle will be discussed.

5.Mass Flow Rate Enhancement

Two basic principles to improve wind turbine efficiency have been indicated in the past. The first principle is to increase the mass flow rate of the wind turbine while the second principle is to generate turbulent mixing of the wake behind the rotor (Hutter, 1977). The first principle is best explained in Figure 3 below.

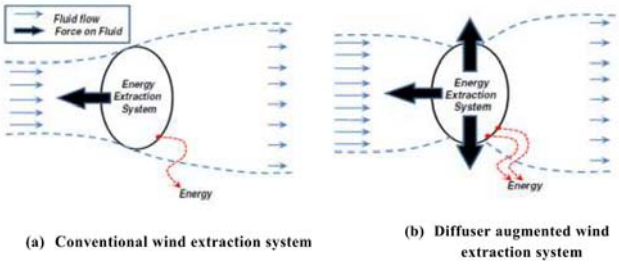

Figure 3. Wind Energy Extraction Systems (Hoopen, 2009)

The flow deceleration causes pressure increase in front of the rotor that leads to a fraction of the mass flow being pushed sideway around the rotor. The force pushing the flow sideway is perpendicular to the fluid flow, which can be realised by placing a shroud around the rotor. Exerting the perpendicular force with an annular lifting shroud is one of the ways to boost the velocity across the rotor. An annular lifting shroud functions as a suction device that points the lifting force towards the centre. From the third law of Newton, the wind flow will create a reaction force to counteract the lifting force in order to establish force equilibrium. The counteracting force produced by the wind flow results in a huge amount of air mass being sucked through the annular lifting shroud. As such, the counteracting force will widen the stream tube and thus augment the wind velocity.

Based on this concept, a Computational Fluid Dynamic (CFD) simulation was performed to design an annular lifting

device (Bet & Grassman, 2003). As illustrated in Figure 4 (a), with the addition of an airfoil shroud around the rotor, the low pressure region behind the wind turbine is significantly enlarged. In contrast with Figure 4 (b), a further enlargement on the low pressure region can be achieved by adding a secondary wing shroud around the first shroud. It was reported that their DAWT showed an increase in power output by the wing system by a factor of 2, compared to the un-shrouded wind turbine, thereby exceeding Betz limit (1966).

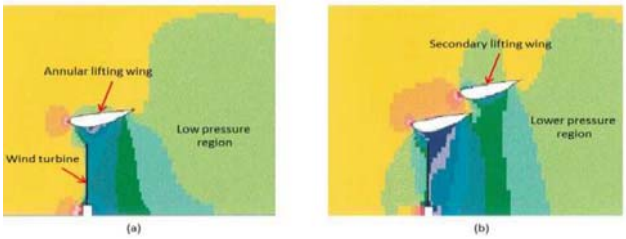

Figure 4. CFD Simulation Showing Static Pressure around Propeller With Single and Secondary Annular Lifting Wing Added Around Wind Turbine (Bet & Grassman, 2003).

Many researches on the examination of a diffuser augmented wind turbine (DAWT) were carried out intensively in the past. A conclusive fact by Kogan and Seginer (1963) in their final report is that the sub-atmospheric pressure at the exit plane of a shrouded rotor and around the rotor will directly affect the power augmentation of a shrouded rotor, as the sub-atmospheric pressures create a suction effect and therefore result in higher mass flow. With this concept, Igra (1981) researched on the pressure difference of shrouded rotor with many different types of diffuser. From his experimental work, he deduced that a high efficiency diffuser should keep the exit pressure as low as possible and the area ratio as big as possible. The area ratio is the ratio of the diffuser entrance and exit plane area relative to the swept rotor area. On the other hand, scientists like Foreman, B.Gilbert, and Oman (1977), focused on concentrating wind energy in a diffuser with a large open angle, the flow that goes along the inside surface of a diffuser is governed by a boundary layer controlled with several flows slots. Thus, the method of boundary layer control prevents pressure loss by flow separation and increases the mass flow inside the diffuser.

Departing from this idea, a group of researchers from New Zealand developed a boundary-layer-control-diffuser, named the Vortec 7 (Phillips, Flay, & Nash, 1999). A multi-slotted diffuser was used to prevent separation within the diffuser. From the experimental research conducted on this system, it was shown that a Vortec 7 wind turbine generated more power compared to a un-shrouded wind turbine, with a power coefficient four times higher (Philips, Richards, & Flay, 2006). It is also shown that with the use of diffuser, the vortex structure flow on the downstream of un-shrouded wind turbine can be easily dispersed, which is another important characteristic that assists the wind energy capture of a wind turbine.

Another group of researchers in UK designed a three-sections-nozzle-cylinder-diffuser accelerate system to improve the mass flow rate across the rotor. It was found that the wind speed in the system is significantly influenced by the length of the cylinder as well as the shape of inlet and outlet. With proper inlet, outlet design and optimal length of these sections, wind speed enlargement can be achieved (Wang, et al. Wang, Bai, Fletcher, Whiteford, & Cullen, 2008).

6.Wind-lens Technology

Wind-lens turbine is a newly developed wind turbine system that not only adopts a diffuser-shaped structure similar to other turbines, but a large flange is also attached at the exit of the diffuser shroud. The flanged structure is called 'wind-lens', which was developed by Ohya, Karasudani, Sakurai, Abe, and Inoue (2008), from Kyushu University in Japan. This idea consisted of a combination of the two basic principles of power enhancement mentioned earlier. Several research and testing have been done in Kyushu University and Sasebo National College of Technology. It was proven in the field test conducted by Ohya, Karasudani, Ngai, Chris, and Griffiths (2011) that the wind-leans was able to increase the power augmentation by a factor of about 4 times, for a given wind speed and wind turbine diameter.

Simulation results done by Bet and Grassman (2003) have shown a significant increase in the coverage of low pressure region behind the rotor. In light of this fact, this group of researchers formed an idea of a flange design, which is also called a broad brim design. Due to a strong vortex formation behind the flange, huge amount of mass flow can be drawn to the wind turbine inside the shrouded diffuser. Hence this new wind turbine system is likely to exceed the Betz limit (Toshinitsu et al., 2008). Owing to this effect, the power generated from wind can be increased to a greater amount. This is because a low pressure region at its downstream will accelerate the moving air when passing through the rotor. As a result, more power can be extracted. Figure 5 gives a detailed image on the flange design.

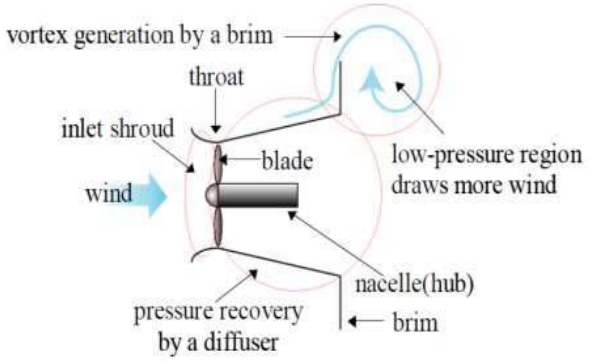

Figure 5. Schematic View of Flow Mechanism around a Flanged Diffuser (Jha, 2011).

B. *Decisive Factors on Shroud Design*

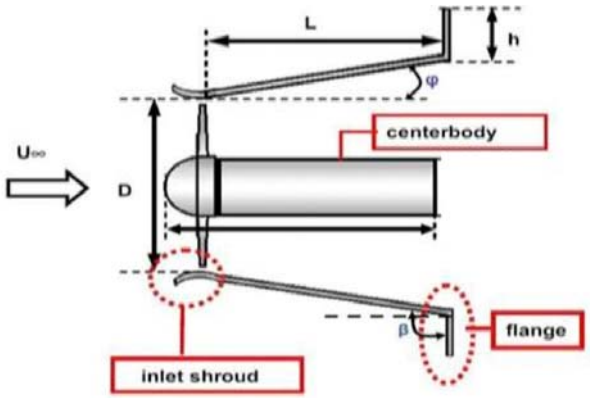

Figure 6. Parameters Employed on Design a Diffuser Shroud (Ohya et al., 2008)

Figure 6 shows the parameters involved in the design of a diffuser shroud. Meanwhile, the parameters considered in the project are listed and described in Table 1.

TABLE I. PARAMETERS OF DIFFUSER SHROUD

Symbol	Description
L	Length of diffuser shroud
D	Inlet diameter of diffuser shroud
h	Width of the flange: angle from diffuser wall to the horizontal
ϕ	Expansion angle of entrance
β	Tilt angle of flange: angle from flange to the horizontal

C. *Diffuser Shroud Design*

It was found by Matsushima et al. (2006) that significant wind speed enhancement can be achieved when the ratio of length on diameter (L/D) is more than a factor of 3. However, in designing a wind energy capturing device that is feasible to be placed on the rooftop of a car, the size of the device is one of the important design criteria. A long length diffuser shroud tends to enhance power extraction, yet is not practical for a vehicle equipped with a wind energy capturing device. Recent research done by Ohya and Karasudani (2010) concluded that with a proper flange design and a lower L/D ratio, as low as 1.5, a similar performance level can be achieved. Aside from the design of the diffuser shroud, the design of the flange is also influential. It was confirmed that maximum performance can be achieved when the ratio of flange width on inlet diameter (h/D) is between 0.25 to 0.5 (Ohya & Karasudani, 2010).

In general, the rooftop of a conventional family car has an approximate length of 1.8 m and width of 1.5 m, so the shroud must be designed within the span of rooftop. Moreover, this design aspect must be taken into account for safety reasons too. Having that in mind, the length of the diffuser shroud was adopted to be L = 600 mm which is one third of rooftop length.

D. *Flange Design*

The philosophy behind having a flange at the exit periphery of the diffuser shroud is to create a lower pressure region at the downstream to boost the velocity of incoming air. Previous research done on flange diffuser shrouds only considered the effects of the width of the vertical flange. As such, it was interesting to find out how the tilt angle (β) of the flange can influence the pressure region at the downstream and how the change in flange profile could lead to a velocity enhancement. The effects of change in tilt angle and flange profile were simulated in a numerical analysis, which will be discussed later. Table 2 summarises the important parameters from literature on designing a diffuser shroud and its respective initial adopted values.

TABLE II. GEOMETRY PARAMETERS FOR DIFFUSER SHROUD AND INITIAL ADOPTED VALUES

Parameters	Range	Initial Adopted Value
L/D	1.5 – 3	1.5
h/D	0.25 - 0.5	0.25
D'/2R	1 -1.3	1.15
ϕ	4°-6°	4°
β	N/A	90°

Note: D' is the projected diffuser diameter corresponding to the wind turbine's location.

III. DESIGN AND PROCUREMENT

This section demonstrates the numerical analysis of several configurations of a diffuser shroud using ANSYS 13.0 computational fluid dynamics (CFD). The simulation results can be used to illustrate the performance of the flow and resemblance of the flow. Out of the many generated models, the one with the best performance was selected for manufacturing.

A. *Validation of CFD Method*

A fluid CFD simulation model identical to one of the models developed by Ohya et al. (2008) was replicated for the purpose of setup validation. Velocity characteristics along the central axis of the diffuser model was analysed to confirm the steps taken in constructing the CFD simulation. Figure 3 plots a comparison between the results obtained by CFD and the experimental result done by Ohya et al. (2008) in terms of the wind-speed ratio (U/U∞) and length ratio (x/L), where x/L = 0 is the model entrance and x/L = 1 is the model exit. Wind-speed ratio is the ratio of the speed at an arbitrary location and the free stream velocity, while length ratio is a ratio at an arbitrary distance x measured from the diffuser shroud entrance and the diffuser length (L). The free stream velocity was set to be 10 m/s.

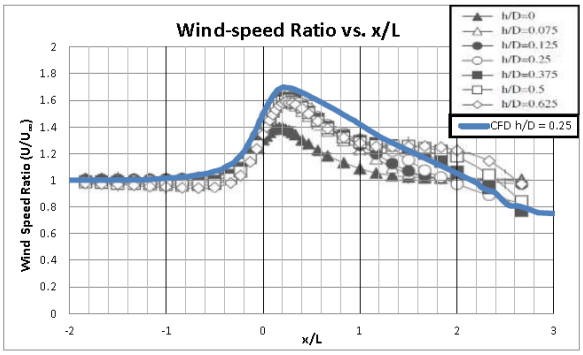

Figure 7. Plots of Comparison Between Result Obtained By CFD and the Experimental Result Done By Ohya et al. (2008).

As illustrated in Figure 7, the result obtained from the CFD analysis shows a similar trend to the experimental result by Ohya et al. (2008). The wind-speed ratio started at 1, and then increased intensely when then flow approached the diffuser entrance ($-1 < x/L < 0$). This phenomenon implied that wind flow was inhaled and accelerated by the diffuser. The speed ratio had a maximum value of 1.7 and was identified at a location approximately $x/L = 0.2$ from the inlet.

However, in the region just after the peak, a difference was found between the numerical results. In this region, the numerical result showed a gradually decrease of wind-speed ratio whereas the experimental results showed a severe drop down . This may indicate that the computational results only showed the ideal patterns of the flow, while the experimental results might be affected by the excessive active turbulent wake behind the flange.

After validating the CFD method, five diffuser models with different tilt angles were simulated in CFD with similar boundary conditions. Figure 8 shows that the wind-speed ratio of these models exhibited similar behavior although the tilt angles (β) were varied. The rapid increase of velocity was observed when flow approached to the diffuser shroud ($-1 < x/L < 0$). It further experienced a slight increase after the entrance ($x/L = 0$) before slowing down towards the exit ($x/L > 1$).

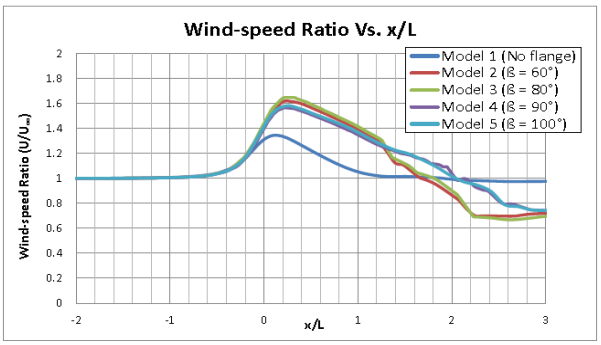

Figure 8. Wind-speed Ratio of Different Models along the Central Axis of Each Model

Even so, discrepancy among these models became obvious after the exit downstream. Firstly, wind flow along Model 1 (No flange) slowed down to its initial speed immediately after the exit, while wind flow along the other models further decreased to a ratio of smaller than 1. Secondly, the trend of wind-speed ratio of Model 1 appeared smoothly and steady after the exit while the trends of the other models are irregular and shaky. These two observations led to a conclusion that vortices are always produced when a flange is present regardless the change in tilt angle of flange.

Furthermore, it was noticeable from Figure 8 that Model 2 and 3, where the angles were tilted forward ($\beta = 60° \& 80°$), had the highest wind-speed ratio out of these models. This implies that the strongest vortices were produced near the exit periphery of these two models and thus the highest velocity occurred. It was concluded that the stronger the vortices near the exit, the higher the velocity can be achieved inside the diffuser shroud. It can also be deduced from this phenomenon that the sharper the angle is, the more active the vortices generated at the exit periphery.

Table III summarizes the maximum wind-speed ratio in each model. It was discovered that the location of maximum velocity shifts away from the entrance when a flange is used. Conversely, when a flange with a different tilt angle was used , the location of maximum wind speed did not change much.

TABLE III. MAXIMUM WIND-SPEED RATIO OF EACH MODEL

Model	U/U_∞, max	Distance from inlet (mm)
Model 1 (No Flange)	1.34	56.38
Model 2 (β o =60°)	1.62	174.50
Model 3(β o =80°)	1.65	145.94
Model 4(β o =90°)	1.57	137.03
Model 5(β o =100°)	1.58	140.94

In this simulation, velocity improvement of the tilted flange-diffuser was found to be similar to the conventional flanged-diffuser (Model 4), specifically, the change in tilt angle does not magnify the pressure difference achieved by a conventional flanged diffuser shroud which was already in use (Ohya et al., 2008).

B. Curved flange Profile Design

On the other hand, changing the profile of the flange may lead to velocity enhancement. Designated Model 6, a new diffuser was replicated by modifying the conventional flange design to a curved flange that has a concave curvature inwards to the diffuser body with a radius of approximately 66 mm. The cross-sectional view and the isometric view of Model 6 (curved flange) are shown in Figure 9 and Figure 10 respectively.

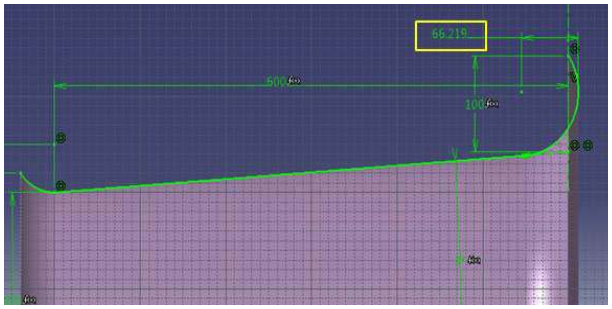

Figure 9. Cross-sectional View of Model 6 (Curved flange)

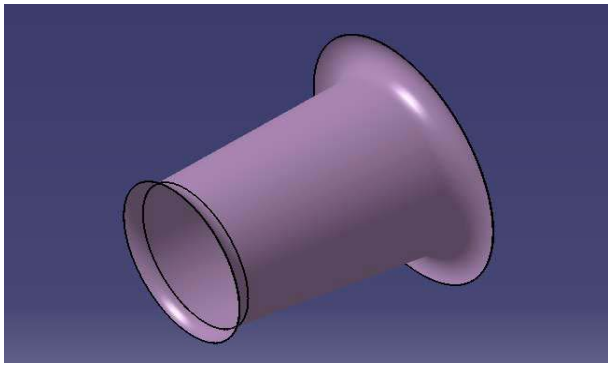

Figure 10. Isometric View of Model 6 (Curved flange)

C. Additional Boundary Conditions

Similarly, a simulation was done on Model 6 with the identical boundary conditions as prescribed in the other models. In addition, a lower approaching wind speed of 5 m/s was also applied at the upstream in the second analysis in order to determine its performance at a low Reynolds number.

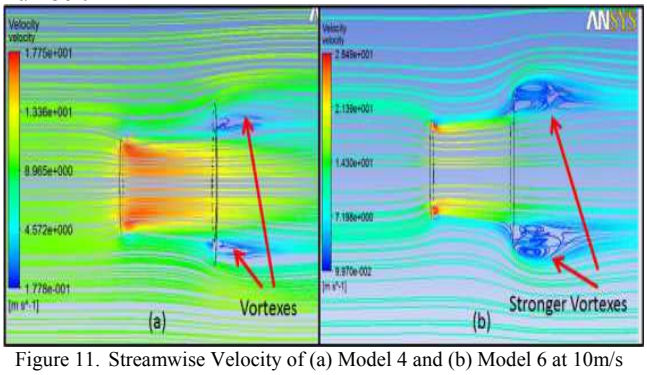

Figure 11. Streamwise Velocity of (a) Model 4 and (b) Model 6 at 10m/s

As indicated in Figure 11 above, stronger vortices were formed with the use of the curved flange in comparison with Model 4 ($\beta = 90°$). This is a result of the pressure difference before and after the flange, which have been magnified by the introduction of a curve profile.

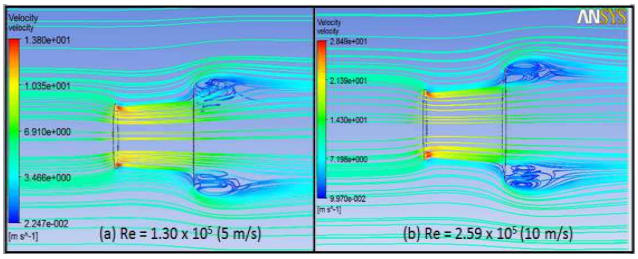

Figure 12. Formations of Vortices at Different Reynolds Number on Model 6

The formation of vortices at different Reynolds number was shown in Figure 12 for a side-by-side comparison. It can be seen that the change in Reynolds number has little effect to the formation of vortices. Similarly, Figure 13 shows that the maximum wind-speed ratio of Model 6 achieved was approximately 2 times higher compared to the free stream velocity regardless of the Reynolds number. This achievement was not only superior to the other models, but also surpassed the maximum wind-speed ratio (1.7) obtained by Ohya et al. (2008).

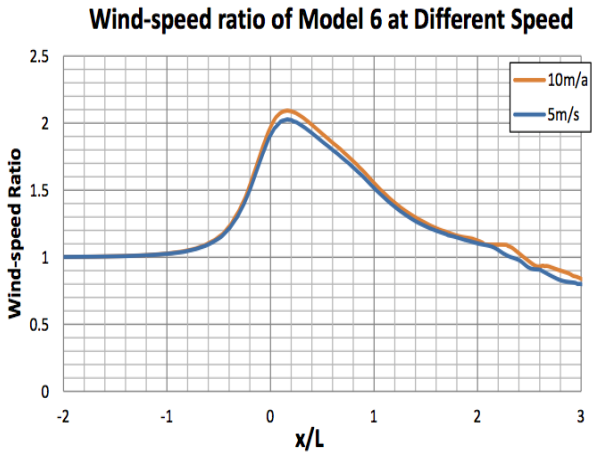

Figure 13. Wind-speed Ratio of Model 6 at Different Reynolds Number

As can be found in Figure 14, the peak value of C_p coincides with the maximum wind-speed ratio along the central axis of diffuser, which implies that highest velocity occurred when C_p was lowest. It is also indicated that the higher the desired velocity is, the lower the pressure must be produced.

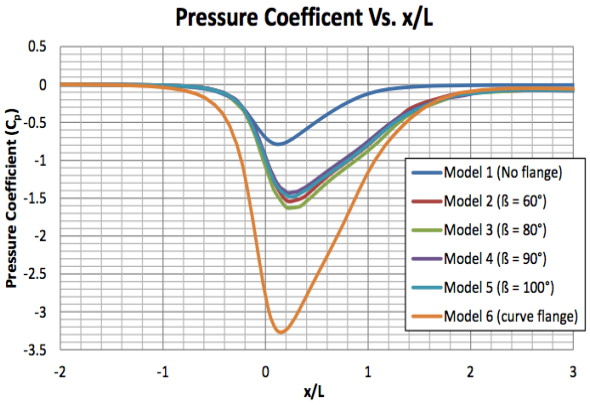

Figure 14. Pressure Coefficient vs. x/L of Different Models

Further analysis with a wind turbine was conducted in Transient Analysis CFD. The simulation investigated the performance of the wind turbine before and after the presence of the curve-flanged diffuser (Model 6). It was found that the power coefficient of the shrouded wind turbine was 1.48, which exceeded the Bitz limit (1966) of 0.59. The mechanical power was also enhanced by approximately 3 times. As such, Model 6 was the best to be fabricated and tested in laboratory. Henceforth, the diffuser shroud mentioned in following sections refers to Model 6 diffuser.

IV. Experiment and Results

A. Experiment Setup

The interest of this experiment was to find out the enhancement of incoming velocity along the central axis of the diffuser shroud as well as the augmentation of mechanical power of a wind turbine before and after the diffuser shroud was equipped. The free stream velocity was produced by an open wind tunnel. It remained at 5m/s when testing for incoming velocity enhancement and was gradually increased from the cut-in speed the wind turbine to 15m/s with an interval of 1.5m/s during the test for power augmentation. A hot-wire anemometer, load transducer and a digital tachometer were used to obtain experimental data.

Figure 15. Laboratory Setup for Enhencement of Power Augmentation

The laboratory setup for Experiment can be seen from Figure 15. It was observed that vibration of the diffuser shroud occurred when the wind speed was greater than 13 m/s. Therefore, the speed range was limited to 10.5 m/s for safety. As discovered from the experiment presented in above section, extreme condition occurred at R = 2 Ω and R = 25 Ω, where maximum power coefficient was produced at R = 25 Ω and maximum electrical power was produced at R = 2 Ω. Therefore, the experiment was conducted for 2 Ω and 25 Ω over the nominal safety speed range.

B. Enhencement of Incoming Velocity Experiment

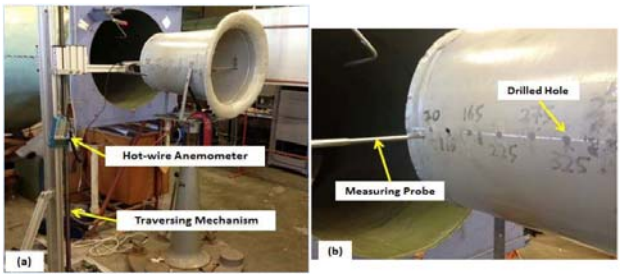

Figure 16. Laboratory Setup for Enhencement of Incoming Velocity Experiment

A uniform wind speed of 5 m/s was used throughout the experiment. As the interest of this experiment was to study the flow field along the central axis of the diffuser shroud, the wind turbine and the supporting brackets were removed. This experiment also required the use of a hot-wire anemometer and traversing mechanism.

The traversing mechanism placed at the side of diffuser shroud can be seen in Figure 16(a), while the measuring probe of hot-wire anemometer was slotted into the drilled holes is shown in Figure 16(b).

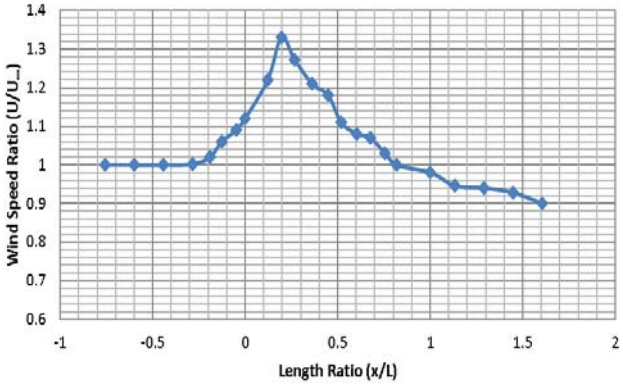

Figure 17. Plot of Wind-speed Ratio vs. Length Ratio of Diffuser Shrouded

Figure 17 explains the flow characteristics along the central axis of the diffuser shroud. As seen far up stream, the wind-speed ratio began at 1 and started increasing at x/L = -0.28. Meanwhile, a wind-speed ratio of 1.12 was measured at the entrance. The continuous increase in wind-speed ratio was found to reach its peak at x/L = 0.196, and the corresponding wind-speed ratio recorded was 1.33. After reaching the peak, the wind speed-ratio gradually decreased towards the exit (x/L = 1). On the other hand, at the downstream region just after the exit (x/L > 1), the wind speed decreased gradually. The explanation for this finding is that after the exit, the energy from the surrounding airstream was transferred to the flow exiting from the diffuser. Therefore, the decreasing effect was not relatively significant to the flow inside the diffuser shroud.

C. *Power Augmentation Experiment*

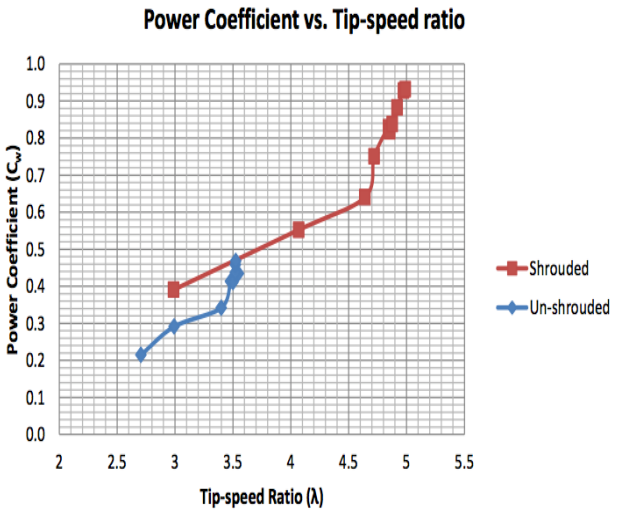

Figure 18. Plot of Power Coefficient vs. Tip-Speed Ratio for Shrouded Case and Un-Shrouded

Figure 18 plots the power coefficient of wind turbine versus the tip-speed ratio for both shrouded and un-shrouded cases. It can be observed that the un-shrouded wind turbine had a narrow range of tip-seed ratio and a lower value of power coefficient compared to the shrouded wind turbine. According to Cetin et al. (2005), the ideal tip-speed ratio for a two-blades wind turbine is 6.3. Moreover, the maximum obtainable tip-speed ratio of the un-shrouded wind turbine was 3.52 while the shrouded wind turbine had a tip-speed ratio of 4.97, which is much closer to the ideal value. A further increase of tip-speed ratio is expected in higher wind speed, but the experiments were halted for safety reason. The enhancement in tip-speed ratio leads to an understanding that the diffuser shroud can optimise the tip-speed ratio of a wind turbine to its ideal operating condition.

Figure 18 illustrates that the un-shrouded wind turbine had a narrow range of tip-seed ratio and a lower value of Power Coefficient (Cw) compared to the shrouded wind turbine. The maximum Cw of the un-shrouded wind turbine was approximately 0.43, which is a typical expected power coefficient for a conventional wind turbine. Whereas the maximum Cw for the shrouded wind turbine had surpassed the Betz limit with a higher value of 0.93. A Cw value close to 1 indicates that almost all the energy in the approaching wind speed was captured. With the data acquired from the load transducer and tachometer, the mechanical power and Cw at $U\infty = 10$m/s were deduced as shown in Table IV.

TABLE IV. POWER COEFFICIENT, MECHANICAL POWER AND POWER AUGMENTATION AT 10M/S

Model	Numerical Analysis	Experimental Results
Un-Shrouded	P = 29.30 Watt Cw = 0.46	P = 31.05 Watt Cw = 0.43
Shrouded	P= 92.26 Watt Cw =1.48	P = 62.92 Cw = 0.93
Power Augmentation	≈ 3 times	≈ 2 times

V. CONCLUSION

From the first experiment, the incoming velocity was accelerated by a factor of 1.33, while the numerical analysis predicted an increased factor of 2.1. The second experiment showed that the diffuser shroud had doubled the mechanical power of the un-shrouded wind turbine. However, in the numerical simulation, the use of the diffuser shroud had in fact augmented the mechanical power of the un-shrouded wind turbine by approximately 3 times. The major contribution to this disagreement of results could be due to the rough surface finish and dimension inconsistency of the manufactured diffuser. In addition, the blockage effect of the open wind tunnel was believed to have a minor effect to this discrepancy as well. In spite of the disagreement between numerical and experimental results, it nevertheless has shown a qualitative agreement with literature.

REFERENCES

[1] Abea, K., & Ohya, Y. (2004). An investigation of flow fields around flanged diffusers using CFD. Journal of Wind Engineeringand Industrial Aerodynamics, 92, 315-330.

[2] Asaf, V., Cumali, I., & Yasin, V. (2001). Increasing the efficency of wind turbines. *Wind Energy* and Industrial Aerodynamic, 89, 809-815.

[3] Bet, F., & Grassman, H. (2003). Upgrading conventional wind turbines. *Renewable Energy, 28*, 71-73.

[4] Betz, A. (1966). *Introduction to the Theory of Flow Machines* (T. D. G. Randall, Trans.). Oxford: Pergamon Press.

[5] Burton, T., Sharpe, D., Jenkins, N., & Bossanyi, E. (2001). *Wind Energy Handbook*. New York: John Wiley & Sons.

[6] Cetin, N. S., Yurdusev, M. A., Ata, R., & Ozdemir, A. (2005). Assesment of optimum tip speed ratio of wind turbines. Mathematical and Computational Applications, 10(1), 147- 154.

[7] David, J. (2008). Diffuser, from http://accessscience.com/content/Diffuser/194100

[8] EIA. (2011). U.S. Energy Information Administration: International Energy Outlook 2011.

[9] EPA. (2007). Air and Radiation Pollusions. Retrieved 22-6-2012, from http://www.epa.gov/air/airpollutants.html

[10] Foreman, K. M., B.Gilbert, & Oman, R. A. (1977). Diffuser augmentation of wind turbine. *Solar Energy, 20*, 305-311.

[11] Green, S. I. (1995). Fluid Vortices: Fluid mechanics and its application - Vortices in aeroporpulsoon systems: Kluwer Academic Publisher.

[12] Hansen, M. O. (2008). *Aerodynamic of wind turbines* (2nd. ed.): London & Sterling VA: Earthscan.

[13] Hau, E. (2006). Wind Turbine - Fundamentals, Technologies, Application, and Economics (2nd ed.). Berlin: Springer.

[14] Hirahara, H., Hossain, M. Z., Kawahashi, M., & Nonomura, Y. (2005). Testing basic performance of a very small wind turbine designed for multi-purposes. *Renewable Energy, 30*, 1279- 1297.

[15] Hutter, U. (1977). Optimum wind energy conversion system. *Annual Review of Fluid Mechanics, 9*, 399-419.

[16] Igra, O. (1981). Research and development for shrouded wind turbines. *Energy Conversion and Management, 21*, 13-48.

[17] Jackson, H. W. (1959). *Introduction to Electronic Circuits*: Prentice-Hall.

[18] Jha, A. R. (2011). *Wind Turbine Technology* (1st ed.). UK: CRC Press.

[19] John, D., & Anderson, J. (2010). *Fundamentals of aerodynamic* (5th ed.): The McGraw Hill Companies.

[20] Kumar, D. S., & Kumar, K. L. (1980). Effect of Swirl on Pressure Recovery in Annular Diffusers. *Journal of Mechanical Engineering Science, 22*(6), 306-313.

[21] Matsushima, T., Takagi, S., & Muroyama, S. (2006). Characteristic of highly efficient propeller type small wind turbine with a diffuser. *Renewable Energy, 31*, 1343-1354.

[22] Ohya, Y., & Karasudani, T. (2010). A Shrouded Wind Turbine Generating High Output Power

[23] with Wind-lens Technology. *Energies, 3*, 634-649.

[24] Ohya, Y., Karasudani, T., Ngai, T., Chris, T. M., & Griffiths, H. (2011). *Development of shrouded*

[25] *wind turbines with wind-lens technology*. Paper presented at the Europe's Premier Wind Energy Event, Brussels.

[26] Ohya, Y., Karasudani, T., Sakurai, A., Abe, K., & Inoue, M. (2008). Development of a shrouded wind trurbine with a flanged diffuser. *Wind Energy Industrial and Aerodynamics, 96*, 524-539.

[27] Philips, D. G., Richards, P. J., & Flay, R. G. J. (2006). Diffuser development for a diffuser augmented wind turbine using computational fluid dynamics, from http://www.cham.co.uk/PUC/PUC_Luxembourg/Presentations/AucklandU_Phillips.doc

[28] Phillips, D. G., Flay, R. G. J., & Nash, T. A. (1999). Aerodynamic analysis and monitoring of the Vortec 7 diffuser-augmented wind turbine. *IPENZ Transactions, 26*(1/EMCh).

[29] Rechenberg, I. (1989). *Development and operational of a novel wind turbine with vortex screw concentrator*. Paper presented at the Second Joint Schlesinger Seminar on Energy and Enviroment, Berlin.

[30] Toshinitsu, K., Nishikawa, K., Haruki, W., Oono, S., Takao, M., & Ohya, Y. (2008). PIV measurements of flows around the wind turbines with a flanged-diffuser shroud. *Journal of Thermal Science, 17*, 375-380.

[31] Wang, F., Bai, L., Fletcher, J., Whiteford, J., & Cullen, D. (2008). The methodology for aerodynamic study on a small domestic wind turbine with scoop. *Journal of Wind Energy and Industrial Aerodynamics, 96*, 1-24.